Developing a joint operation framework for complex multiple reservoir systems

Jinggang Chu, Yu Li, Yong Peng and Wei Ding

ABSTRACT

This study aims to present a joint operation framework for complex multiple reservoir systems to balance water supply between subsystems and between different stakeholders, and support decisions about water releases from the entire system and individual reservoirs effectively. The framework includes three steps: (1) aggregated virtual reservoirs and various subsystems are established to determine the water releases from the entire system; (2) the common water-supply strategy is identified to determine the water releases from individual reservoirs; and (3) the joint operation problem is solved with a multi-objective optimization algorithm and the results are analyzed using a Many-Objective Visual Analytics Tool (MOVAT). A case study of the DaHuoFang-GuanYinGe-ShenWo multi-reservoir system in northeastern China is used to demonstrate the framework. Results show that the establishment of aggregated virtual reservoirs and identification of a common water-supply strategy could make use of the temporal and spatial differences of runoff, exert the effects of underlying hydrological compensation between river basins, and reduce the complexity of the joint operation model for multiple reservoir systems effectively. The MOVAT provides an effective means of solving many-objective problems, which are generally of particular concern to the decision-maker in practice.

Key words | many-objective algorithms, multi-reservoir systems, tradeoff, visual analytics, water supply

Jinggang Chu
Yu Li (corresponding author)
Yong Peng
Wei Ding
School of Hydraulic Engineering,
Dalian University of Technology,
Dalian 116024,
China
E-mail: *dagongliyu@qq.com*

INTRODUCTION

Multi-reservoir systems play an important role in water resource management. The coordinated operation of multi-reservoir systems is typically a complex decision-making process involving many variables, many objectives, and considerable risk and uncertainty (Oliveira & Loucks, 1997; Xu *et al.* 2014; Zhang *et al.* 2014). Optimally scheduling multi-reservoir systems should make use of temporal and spatial variations of runoff, the underlying hydrological compensation between river basins and operation compensation between reservoirs, and thus improve the overall performance of the system in terms of the optimal allocation of water resources (Zhang *et al.* 2012; Zhu *et al.* 2014, 2015).

Operating rules for multi-reservoir systems must specify not only the total release from the system but also the amounts of water to be released from each reservoir. The literature on the development of operating rules for multi-reservoir systems is extensive. For reservoirs in series, the Water Storage Rule (or Sequence Rule) is often used (Lund & Guzman 1999), that is, the water in downstream reservoirs should be used before upstream reservoirs, which is based on compensation adjustment. In the parallel reservoirs system, the New York City rule (NYC rule) (Clark 1950) and the space rule (Bower *et al.* 1962) have been widely used. The NYC rule equalizes the probability of filling each reservoir, while the space rule seeks to leave more space in reservoirs where greater inflows are expected to minimize water shortage in future. However, they cannot provide clear indications on how to operate complex systems that

doi: 10.2166/ws.2015.105

have separate demands from individual reservoirs, joint demands, several purposes and tight constraints (Lund & Guzman 1999).

Johnson *et al.* (1991) modified the space rule to consider the existence of separate demands, which attempts to make the available, active storage space in each reservoir proportional to its cumulative expected inflow minus separate demands (Oliveira & Loucks 1997). Wu (1988) described a rule that attempts to keep the storage volume of each reservoir proportional to the expected net separate demand during the remainder of the drawdown season. However, these improved rules employ the standard operating policy (SOP) which releases as much as the demand if there is enough water. In addition, these rules use the cumulative expected inflow with uncertainty in the refill season. Finally, they only consider minimizing water shortage in the whole system, neglecting balances between subsystems and between different stakeholders. Thus there is a need to develop a joint operation model for complex multiple reservoir systems that explicitly considers the various trade-offs mentioned above.

Explicitly considering tradeoffs between many objectives can help avoid decision biases of different stakeholders in complex planning problems (Brill *et al.* 1982). Many-objective optimization algorithms can reveal objective tradeoffs in which a sacrifice of one benefit is required for the gain of other benefits. Tradeoffs can be illustrated with advanced visual analytic tools, which allow richer information to be explored in a more intuitive way, yield new design insights and avoid the potentially highly negative consequences. Many-objective visual analytics have been used in water-supply risk management (Kasprzyk *et al.* 2009), groundwater monitoring network design (Kollat & Reed 2006; Kollat *et al.* 2011), water distribution system optimal design (Fu *et al.* 2012, 2013), wastewater system control (Fu *et al.* 2008; Sweetapple *et al.* 2014) and reservoir operation (Hurford *et al.* 2014).

This paper aims to present a joint operation framework for the complex multiple reservoir system to derive the optimal releases from the entire system and each individual reservoir. The DHF-GYG-SW multi-reservoir system, which consists of DaHuoFang reservoir (DHF), GuanYinGe reservoir (GYG) and ShenWo reservoir (SW), is used as a case study. After establishing aggregated virtual reservoirs and identifying the common water-supply strategy, a joint operation problem for the complex multiple reservoir system is built and solved with a multi-objective optimization algorithm, i.e., ε-NSGAII (Kollat & Reed 2006), to obtain approximate Pareto optimal solutions. Many-objective visual analytics (Kasprzyk *et al.* 2009; Fu *et al.* 2013) are used to explore the tradeoffs between conflicting objectives, and provide an understanding of the derived optimal releases. Multi-objective analysis is demonstrated as one way forward to address the challenges identified in optimal operation of multi-reservoir systems, particularly in revealing and balancing the conflicts between different stakeholders.

MATERIAL AND METHODS

Study area

The DHF-GYG-SW multi-reservoir system is located in the Huntai basin, which is a rapidly urbanizing region of northeast China (Figure 1).

The DHF-GYG-SW multi-reservoir system was built mainly for the purposes of industrial water supply, agricultural water supply and environmental water supply. In particular, the environmental water demand should be satisfied fully according to regulations (Zhu *et al.* 2014). The multi-reservoir operation system has many features and challenges typical of real-world reservoir systems. The reservoir characteristics, annual average inflow, water-supply tasks, operation rules, inflow and water demand data used in this study are provided in the Supplementary Material (available in the online version of this paper).

Aggregated virtual reservoirs

The aggregation–disaggregation approach, which aggregates multi-reservoir systems into a virtual reservoir for making decisions on water supply, could reduce the dimension and computational complexity, and is regarded as an efficient way to perform joint scheduling for a multi-reservoir system (Oliveira & Loucks 1997; Archibald *et al.* 2006; Liu *et al.* 2011; Xu *et al.* 2014). Thus it is used in this study. The entire multi-reservoir system consists of three subsystems, shown in Figure 1. Each subsystem has different water sources and demands, which should be met with different

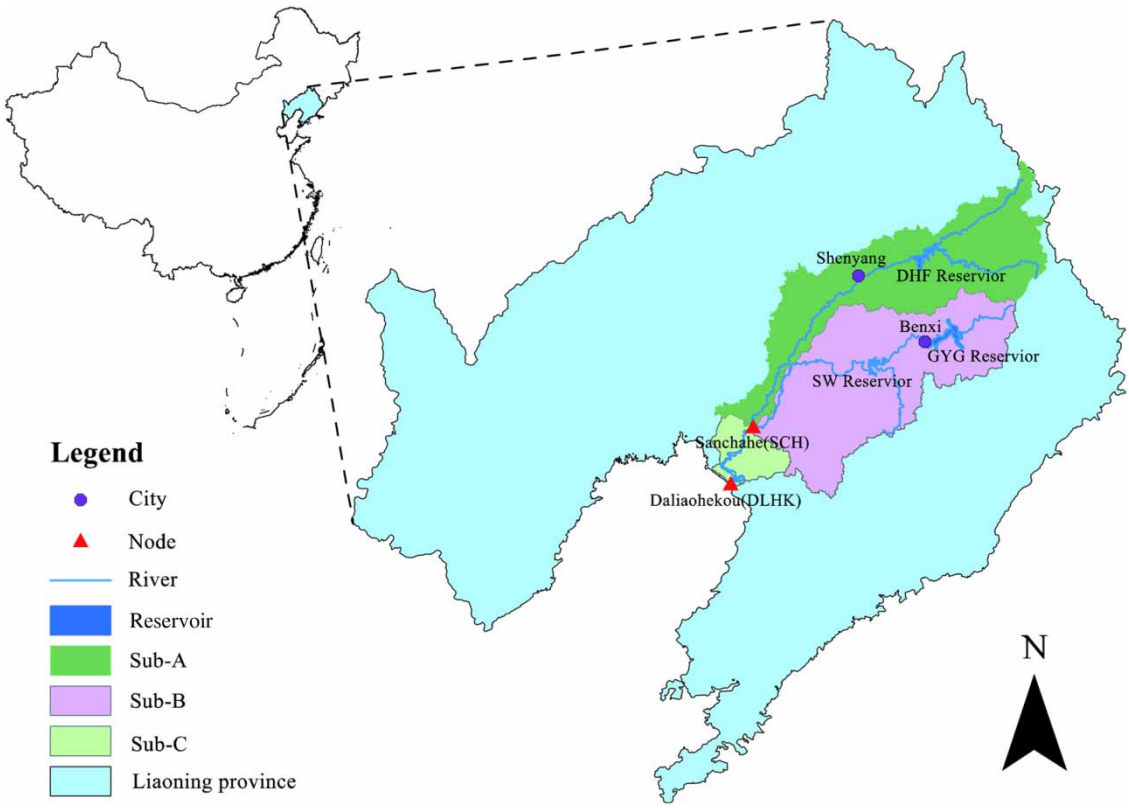

Figure 1 | The location of the multi-reservoir system.

degrees of reliability. The reservoirs GYG and SW in subsystem Sub-B are aggregated into one virtual reservoir (XN-2). Similarly, the reservoirs DHF, GYG and SW are aggregated into another virtual reservoir (XN-3).

Common water-supply strategy

Another step in using the aggregation–disaggregation approach is disaggregation, which indicates the amounts of water to be released from each reservoir and is related to the common water-supply strategies.

In reservoir XN-2, GYG and SW are reservoirs in series, and SW is located downstream of GYG. The active capacity and storage coefficient of GYG are about 2.7 times and 3.6 times those of SW, respectively, when inflow into GYG is less than that into SW. The Water Storage Rule could be employed for the common water supply of the XN-2 reservoir. However, due to the separate demands of GYG, GYG cannot recharge SW unrestrictedly, and the Water Storage Rule is modified by adding the limit curve of supply in the GYG reservoir to avoid oversupply.

XN-2 is combined with DHF in parallel to make reservoir XN-3, which supplies water to the SCH-DLHK interval. The water supply of XN-3 should be distributed to XN-2 and DHF. We adopted the common water-supply strategy in which the total water supply is distributed to each reservoir proportionally to its expected inflow plus current storage minus separate demand. The proportion of water-supply distribution is calculated using

$$K_{i,t} = \frac{S_{i,t} + I_{i,t} - SD_{i,t}}{\sum_i^N (S_{i,t} + I_{i,t} - SD_{i,t})} \quad (1)$$

where $S_{i,t}$ is the initial water storage of reservoir i at the beginning of period t; $I_{i,t}$ is the inflow into reservoir i during the period t; $SD_{i,t}$ is the separate demand of reservoir i at the beginning of period t; N is the number of reservoirs assuming common water supply.

Optimization model

The optimization problem is formulated as a four-objective optimization problem that seeks to minimize water spills for the entire system (WSP), the water shortage index for Sub-A (SIA), the water shortage index for Sub-B (SIB), and the water shortage index for Sub-C (SIC):

$$\begin{cases} \min f_A(x) = SIA = \omega_{agr}\dfrac{100}{N}\sum_{j=1}^{M}\left(\dfrac{D_{A,agr,j}-W_{A,agr,j}}{D_{A,agr,j}}\right)^2 + \omega_{ind}\dfrac{100}{N}\sum_{j=1}^{M}\left(\dfrac{D_{A,ind,j}-W_{A,ind,j}}{D_{A,ind,j}}\right)^2 \\ \min f_B(x) = SIB = \omega_{agr}\dfrac{100}{N}\sum_{j=1}^{M}\left(\dfrac{D_{B,agr,j}-W_{B,agr,j}}{D_{B,agr,j}}\right)^2 + \omega_{ind}\dfrac{100}{N}\sum_{j=1}^{M}\left(\dfrac{D_{B,ind,j}-W_{B,ind,j}}{D_{B,ind,j}}\right)^2 \\ \min f_C(x) = SIC = \omega_{agr}\dfrac{100}{N}\sum_{j=1}^{M}\left(\dfrac{D_{C,agr,j}-W_{C,agr,j}}{D_{C,agr,j}}\right)^2 + \omega_{ind}\dfrac{100}{N}\sum_{j=1}^{M}\left(\dfrac{D_{C,ind,j}-W_{C,ind,j}}{D_{C,ind,j}}\right)^2 \\ \min f_S(x) = WSP = \dfrac{1}{N}\sum_{j=1}^{M} SU_j \end{cases} \quad (2)$$

where x is the decision variable vector denoting the water-supply rule curves; SIA, SIB and SIC are the shortage indices for Sub-A, Sub-B and Sub-C, respectively, which represent the frequency and quantity of annual shortages that occur during M years, and are adopted as the indicator to reflect water-supply efficiency for the water demand; M is the total number of sample years; $D_{A,agr,j}$ and $D_{A,ind,j}$ are the sum of the target agricultural and industrial water demands in subsystem A during the jth year, respectively; $W_{A,agr,j}$ and $W_{A,ind,j}$ are the sum of delivered water for the agricultural and industrial water demands in subsystem A during the jth year, respectively; $D_{B,agr,j}$, $D_{C,ind,j}$, $W_{B,agr,j}$ and $W_{C,ind,j}$ correspond to the similar terms for Sub-A. The ω terms are the weighting factors, i.e., $\omega_{agr} = 1/3$, $\omega_{ind} = 2/3$. SU_j is the sum of water spill from the entire water-supply system during the jth year.

The decision variables, constraints and the description of the optimization algorithm (ε-NSGAII) used in this paper are provided in the Supplementary Material (available in the online version of this paper).

RESULTS AND DISCUSSION

Because of the random nature of genetic algorithms, eight random seed runs were used to find the Pareto-optimal solutions. For each random seed, the algorithm was run for one million evaluations. Visual analysis showed that beyond one million evaluations there was little improvement in the Pareto approximate sets attained. The Pareto approximate set analyzed in this study was generated across all seed runs. The global view of the tradeoff surface is provided in the Supplementary Material (available in the online version of this paper).

Tradeoffs among subsystems and the entire system

The Pareto approximate set obtained from the full four-objective problem contains all of the solutions for the sub-problems, i.e., three three-objective optimization problems, six two-objective problems, and four single-objective problems. This allows the analysis of the solution sets from lower-dimensional problem definitions with the results from the full four-objective optimization.

The tradeoffs between subsystems and the entire system are shown in Figure 2. In Figure 2(a), both the tradeoffs and positive correlation between SIA and WSP can be observed. As water shortage indices, SIA, SIB and SIC increase with the decrease of water for different subsystems. As mentioned above, Sub-A is supplied only by DHF, and Sub-C is the common water-supply target of DHF and XN-2 reservoirs. First, when SIA is smaller than 0.41, more water in DHF is supplied to Sub-C with the increase of SIA, i.e., a larger common water-supply task is assigned to DHF to decrease SIC and WSP. As a result, a clear tradeoff curve between SIA and WSP can be observed, and the approximate Pareto front is highlighted with red squares. Additionally, when SIA is smaller than 0.41, other solutions, which are not in the tradeoff curve, are also close to this curve, indicating a strong negative relationship between Sub-A and the entire system. Second,

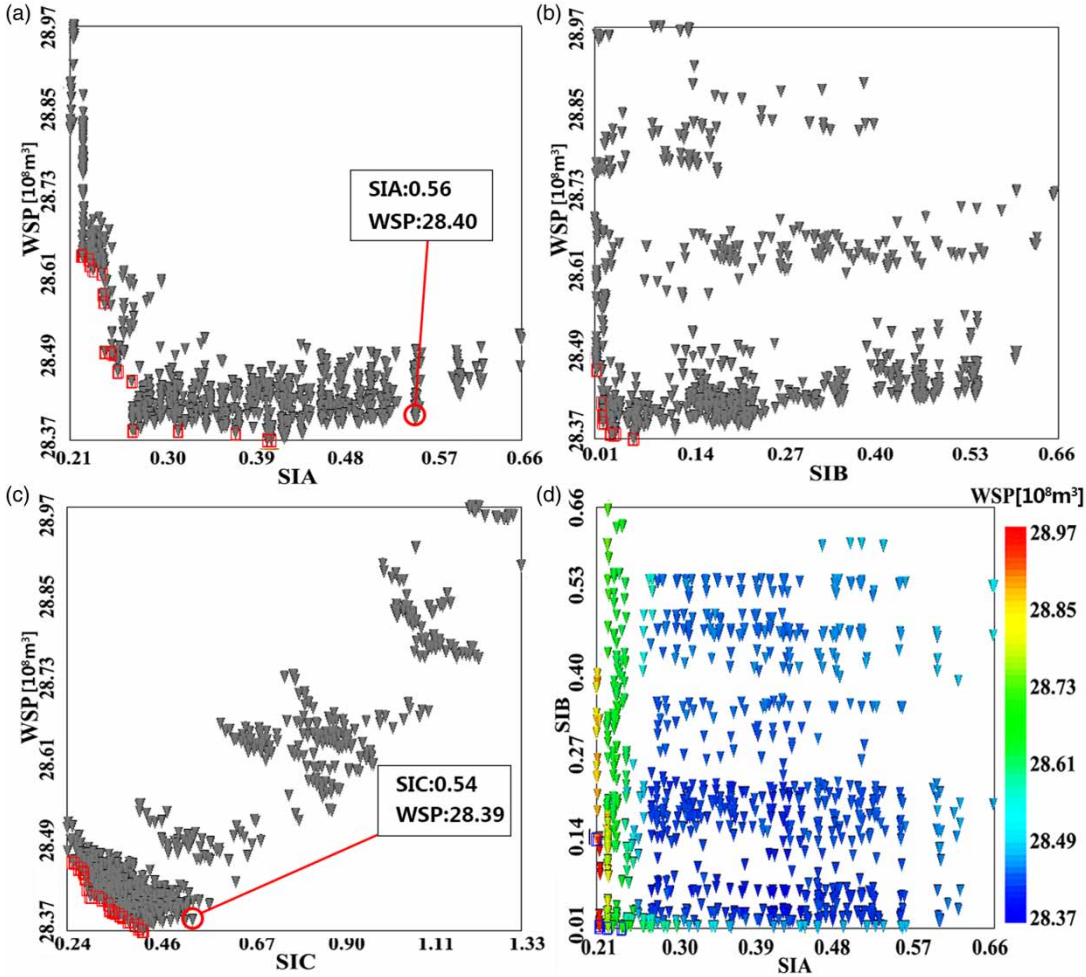

Figure 2 | Tradeoffs between subsystems and the entire system: (a) SIA versus WSP; (b) SIB versus WSP; (c) SIC versus WSP; (d) SIA versus SIB.

when SIA is larger than 0.41, especially larger than 0.56, which is marked in Figure 2(a), more water supplied to Sub-C by DHF could decrease SIC less with the continuous increase of SIA because Sub-C has been satisfied to a large extent. As a result, DHF will spill more water, which leads to an increase in WSP, that is, the two objectives of SIA and WSP present a positive correlation. Thus, the obtained tradeoffs between Sub-A and the entire system are reasonable.

In Figure 2(b), a narrow tradeoff curve between SIB and WSP can be observed and the approximate Pareto front is highlighted with red squares, and it can be observed that most Pareto approximate solutions are far away from this curve, that is, WSP is not sensitive to the variation of SIB. The reason that WSP decreases and then increases with the increase of SIB is similar to that for Figure 2(a).

In Figure 2(c), both the tradeoffs and positive correlation between SIC and WSP can be observed. WSP consists of water spills from Sub-A, Sub-B, and Sub-C. When SIC is smaller (SIC < 0.42), more water is supplied to Sub-A and Sub-B with the increase of SIC to decrease SIA, SIB and WSP. As a result, a tradeoff curve between SIC and WSP can be observed. When SIC is larger than 0.54, marked in Figure 2(c), more water supplied to Sub-A and Sub-B could decrease SIA and SIB less with the continuous increase of SIC because SIA and SIB has been satisfied to a large extent. As a result, spill from Sub-C and WSP will increase, that is, the two objectives of SIC and WSP present a positive correlation. This explains the obtained tradeoffs between Sub-C and the entire system.

Additionally, a narrow tradeoff curve between SIA and SIB can be observed, and the relevant sub-problem

approximate Pareto front is highlighted with black squares in Figure 2(d), where the triangular symbols are shown in colors to represent the WSP objective. First, it is indicated that there is little competition between SIA and SIB; second, the solutions denoted by triangular symbols on the SIA–SIB tradeoff curve have large WSP objective values, close to $28.97 \times 10^8 m^3$, and these solutions are optimal for the sub-systems but not optimal for the entire system; third, it is interesting to note that the Pareto approximate solutions are distributed evenly almost in all ranges of SIA and SIB, and thus an ideal solution would be a blue (less spilled water) triangular symbol, located toward the left lower corner (lower SIA and SIB) of the plot. Therefore, the common water-supply strategy could make use of the temporal and spatial differences of runoff, and the underlying hydrological compensation between river basins effectively and efficiently.

Decision-making with tradeoffs among different subsystems

This section aims to determine the optimal solution based on the tradeoffs among the objectives as discussed above. Interactive visual analytics help decision-makers to understand where performance tradeoffs exist, their severity and shape, especially the inflection points on the tradeoff

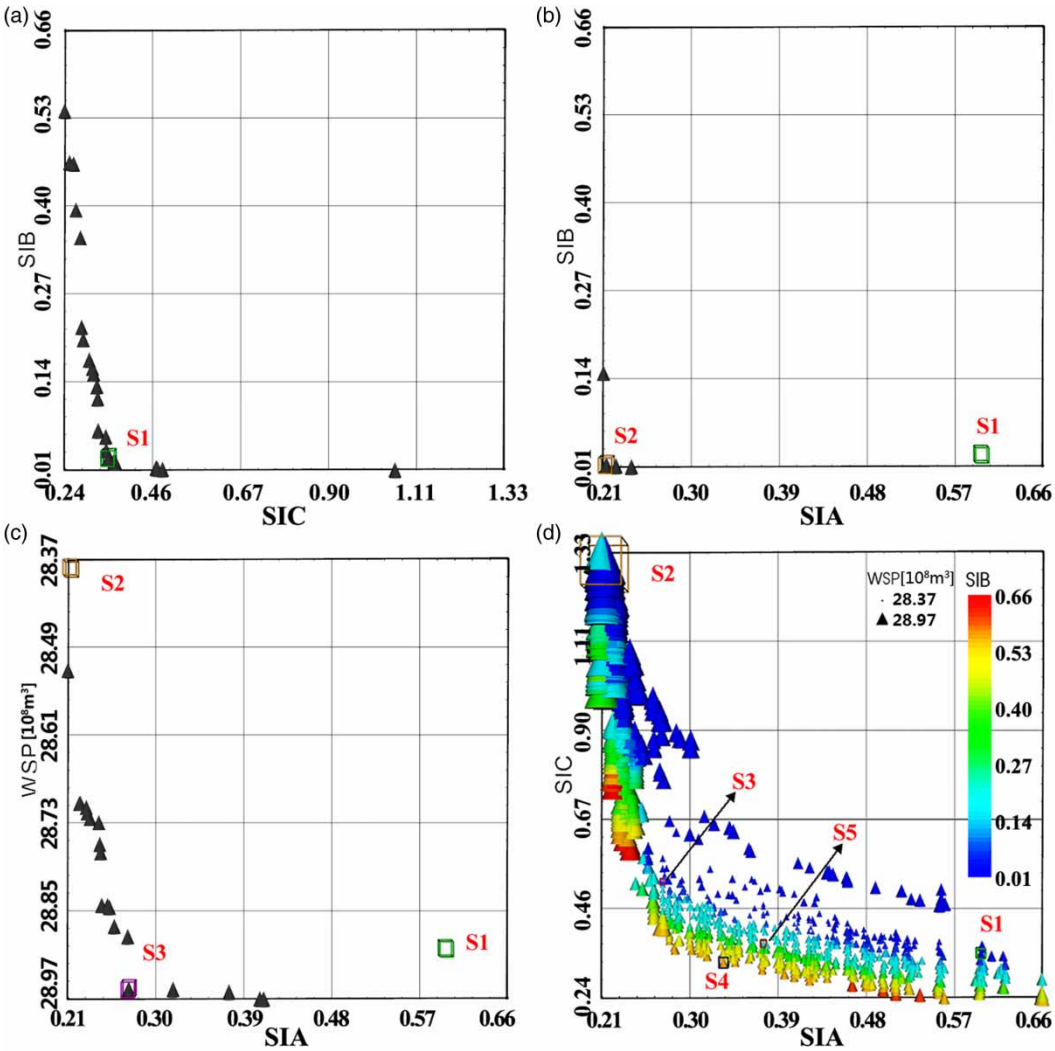

Figure 3 | Decision-making with tradeoffs among different subsystems: (a) SIC versus SIB; (b) SIA versus SIB; (c) SIA versus WSP; (d) global view.

curves, after which the trends are changed. Thus a tool, DecisionVis (Kasprzyk *et al*. 2009; Kollat *et al*. 2011), is used here to explore the solution efficiency in various objectives. Figure 3 shows the decision-making with tradeoffs among different subsystems.

Figure 3(a) shows the tradeoff curve between SIB and SIC. This curve represents the approximate Pareto front had only these two objectives been used for optimization. Considering the tradeoff between the two objectives, a decision-maker might want to choose a solution at the point of diminishing marginal return on the tradeoff curve because after this point there is little improvement in SIB with the increase of SIC. In this way, Solution 1 should be identified and marked with *S*1.

Figure 3(b) shows the tradeoff curve between SIA and SIB. The Pareto approximate solution *S*1 for the SIB–SIC sub-problem highlighted in Figure 3(a) is also shown in Figure 3(b). Because of the larger SIA with *S*1, Solution 2 can be identified at the diminishing point on the SIB–SIA tradeoff curve and is marked with *S*2, which corresponds to a lower SIA and almost the same SIB compared to the SIB–SIC tradeoff curve.

Figure 3(c) shows the tradeoff curve between SIA and *S*1. *S*1 and *S*2 cannot represent the Pareto approximate solutions for the SIA–WSP sub-problem due to their longer distances from the tradeoff curve between SIA and WSP, especially the largest WSP with *S*2. Therefore, Solution 3 is selected at the diminishing point on the SIA–WSP tradeoff curve and marked with *S*3.

In Figure 3(d), SIA and SIC are plotted on the x and y axes, and the SIB objective is shown by colors ranging from red to blue, representing the decreasing preference from 0.66 to 0.01. The WSP objective is represented by the size of the triangular symbols, with large triangular symbols representing more water spill and small triangular symbols representing less water spill. Solution 4 is selected at the diminishing point on the SIA–SIC tradeoff curve and marked with *S*4. In order to balance all objectives, Solution 5 can be identified and marked with *S*5, which is close to *S*4. The reason that *S*5 is selected lies in the following three features: (1) there are lower SIA and SIC compared to *S*1 and *S*2, respectively; (2) in comparison with *S*4, although there are slightly larger SIA and SIC, there are lower SIB and WSP; (3) in comparison with *S*3, there are lower SIC and acceptable increased SIB. However, note that it is difficult to obtain *S*5 with traditional optimization tools because it cannot be intersected by any two-objective tradeoff curves. Therefore, many-objective visual analytics provided an efficient means of solving the many-objective problem, which is generally of particular concern to the decision-maker in practice.

CONCLUSIONS

This paper takes a DHF-GYG-SW multi-reservoir system as an example to present a joint operation framework for the complex multiple reservoir system. With the hierarchical establishment of virtual aggregate reservoirs and identification of a common water-supply strategy, the complexity of the joint operation problem for multiple reservoir systems is reduced, and it is solved with a multi-objective optimization algorithm, i.e., ε-NSGAII. Through the analysis of the tradeoffs among different subsystems and tradeoffs between each subsystem and the entire system using a Many-Objective Visual Analytics Tool (MOVAT), the optimal releases from the system and each reservoir are derived to provide decision support for real-world engineering projects. Results show that the common water-supply strategy in the framework could make use of the temporal and spatial differences of runoff and the underlying hydrological compensation between river basins. Many-objective visual analytics provide an efficient means of solving many-objective problems, which are generally of particular concern to the decision-maker in practice. Therefore, the framework presented in this paper can assist in solving complex decision-making problems in joint operation of the multiple reservoir system.

ACKNOWLEDGEMENTS

This study was supported by the China Postdoctoral Science Foundation Grants (2014M561231) and National Natural Science Foundation of China Grants (51409043). The ε-NSGAII was provided by the MOEA Framework, version 2.1, available from http://www.moeaframework.org/. We

thank Joe Kasprzyk and Patrick Reed for providing valuable assistance in the use of visualization tools.

REFERENCES

Archibald, T. W., McKinnon, K. I. M. & Thomas, L. C. 2006 Modeling the operation of multireservoir systems using decomposition and stochastic dynamic programming. *Naval Research Logistics* **53** (3), 217–225.

Bower, B. T., Hufschmidt, M. M. & Reedy, W. W. 1962 *Operating Procedures: Their Role in the Design of Water-Resource Systems by Simulation Analyses*. Harvard University Press, Cambridge, MA.

Brill, E. D., Chang, S. Y. & Hopkins, L. D. 1982 Modeling to generate alternatives: the HSJ approach and an illustration using a problem in land use planning. *Management Science* **28** (3), 221–235.

Clark, E. J. 1950 New York control curves. *Journal American Water Works Association* **42** (9), 823–827.

Fu, G., Butler, D. & Khu, S. T. 2008 Multiple objective optimal control of integrated urban wastewater systems. *Environmental Modelling & Software* **23** (2), 225–234.

Fu, G., Kapelan, Z. & Reed, P. 2012 Reducing the complexity of multi-objective water distribution system optimization through global sensitivity analysis. *Journal of Water Resources Planning and Management* **138** (3), 196–207.

Fu, G., Kapelan, Z., Kasprzyk, J. R. & Reed, P. 2013 Optimal design of water distribution systems using many-objective visual analytics. *Journal of Water Resources Planning and Management* **139** (6), 624–633.

Hurford, A. P., Huskova, I. & Harou, J. J. 2014 Using many-objective trade-off analysis to help dams promote economic development, protect the poor and enhance ecological health. *Environmental Science & Policy* **38**, 72–86.

Johnson, S. A., Stedinger, J. R. & Staschus, K. 1991 Heuristic operating policies for reservoir system simulation. *Water Resources Research* **27** (5), 673–685.

Kasprzyk, J. R., Reed, P. M., Kirsch, B. R. & Characklis, G. W. 2009 Managing population and drought risks using many-objective water portfolio planning under uncertainty. *Water Resources Research* **45**, W12401, doi:10.1029/2009WR008121.

Kollat, J. B. & Reed, P. M. 2006 Comparing state-of-the-art evolutionary multi-objective algorithms for long-term groundwater monitoring design. *Advances in Water Resources* **29** (6), 792–807.

Kollat, J. B., Reed, P. M. & Maxwell, R. M. 2011 Many-objective groundwater monitoring network design using bias-aware ensemble Kalman filtering, evolutionary optimization, and visual analytics. *Water Resources Research* **47**, W02529, doi:10.1029/2010WR009194.

Liu, P., Guo, S., Xu, X. & Chen, J. 2011 Derivation of aggregation-based joint operating rule curves for cascade hydropower reservoirs. *Water Resources Management* **25** (13), 3177–3200.

Lund, J. R. & Guzman, J. 1999 Some derived operating rules for reservoirs in series or in parallel. *Journal of Water Resources Planning and Management* **125** (3), 143–153.

Oliveira, R. & Loucks, D. P. 1997 Operating rules for multireservoir systems. *Water Resources Research* **33** (4), 839–852.

Sweetapple, C., Fu, G. & Butler, D. 2014 Multi-objective optimisation of wastewater treatment plant control to reduce greenhouse gas emissions. *Water Research* **55**, 52–62.

Wu, R. S. 1988 *Derivation of Balancing Curves for Multiple Reservoir Operation*. Cornell University, Ithaca, NY.

Xu, W., Zhang, C., Peng, Y., Fu, G. & Zhou, H. 2014 A two stage Bayesian stochastic optimization model for cascaded hydropower systems considering varying uncertainty of flow forecasts. *Water Resources Research* **50** (12), 9267–9286.

Zhang, C., Wang, G., Peng, Y., Tang, G. & Liang, G. 2012 A negotiation-based multi-objective, multi-party decision-making model for inter-basin water transfer scheme optimization. *Water Resource Management* **26** (14), 4029–4038.

Zhang, C., Zhu, X., Fu, G., Zhou, H. & Wang, H. 2014 The impacts of climate change on water diversion strategies for a water deficit reservoir. *Journal of Hydroinformatics* **16** (4), 872–889.

Zhu, X., Zhang, C., Yin, J., Zhou, H. & Jiang, Y. 2014 Optimization of water diversion based on reservoir operating rules: a case study of the Biliu River reservoir, China. *Journal of Hydrologic Engineering* **19** (2), 411–421.

Zhu, X., Zhang, C., Yin, J., Zhou, H. & Jiang, Y. 2015 Closure to 'optimization of water diversion based on reservoir operating rules – a case study of the Biliu River reservoir, China' by Xueping Zhu, Chi Zhang, Junxian Yin, Huicheng Zhou, and Yunzhong Jiang. *Journal of Hydrologic Engineering* **20** (7), doi: 10.1061/(ASCE)HE.1943-5584.0001159.

First received 10 February 2015; accepted in revised form 3 July 2015. Available online 21 July 2015